Unraveling the molecular cues of sophorolipid-caped gold-nanoparticle induced ROS stress and apoptotsis-like cell death in Vibrio cholerae

Sristy Shikha
CSIR- Institute of Microbial Technology (IMTECH)
Vineet Kumar
CSIR-Institute of Microbial Technology (IMTECH)
Ankita Jain
CSIR- Institute of Microbial Technology (IMTECH)
Dipak Dutta
CSIR-Institute of Microbial Technology (IMTECH)
Mani Shankar Bhattacharyya (manisb@imtech.res.in)
CSIR- Institute of Microbial Technology (IMTECH)

Research Article

Keywords: Sophorolipid-capped gold nanoparticles, Vibrio cholerae, ROS, antibacterial, oxidative stress

Posted Date: April 26th, 2022

DOI: https://doi.org/10.21203/rs.3.rs-1520875/v1

Abstract

The discovery of nanoparticles exhibiting antimicrobial properties has emerged as one of the most promising therapeutic tools against an array of microbial pathogens. In this study, we investigated the influence of pH, temperature and sophorolipid (SL) concentration on the synthesis of gold nanoparticles. Synthesized sophorolipid capped gold nanoparticles (AuNPs-SL) were checked for antibacterial potential against *Vibrio cholerae*, as well as we investigated the molecular mechanism(s) underlying this activity. We found that AuNPs-SL treatment increases the reactive oxygen species (ROS) level that causes oxidative stress to the bacterial cells. The surge in ROS level further causes membrane depolarization, change in membrane permeability, and ATP depletion. Beside this, gene expression studies revealed overexpression of genes employed in the mitigation of high ROS levels, maintenance of membrane integrity and transport, DNA structure, and metal homeostasis. Furthermore, we also observed cell death (apoptosis) occur as a consequence of AuNPs-SL treatment in *V. cholerae*. Also, AuNPs-SL treatment increases membrane permeabilization that results in leakage of cellular contents such as protein and DNA.

Introduction

The causative agent of cholera, *Vibrio cholerae*, is a genetically versatile, Gram negative, rod-shaped bacterium[1], capable of crossing the acid barrier of the stomach and colonize in the small intestine. They can multiply and secrete the choleragen toxin[2] in the small intestine causing Cholera, the second most leading cause of mortality in children under five years of age and morbidity in adults[3]. Out of the 200 serotypes of *V. cholerae* described, so far, only two; the O1 and the O139 serotypes, are known to be the most virulent. The treatment of cholera primarily includes rehydration therapy, often combined with the administration of antibiotics such as tetracycline, fluoroquinolones, and azithromycin for severe cases[4]. However, in the last few decades, the extensive prescription and overuse of antibiotics has led to the emergence of antimicrobial resistance (AMR) in bacterial pathogens posing a great threat to global health[5]. Therefore, there is an urgent need to change the existing therapeutic strategies to combat these pathogens.

Research outcomes in the past two decades have established the nanoparticles as an alternative drug delivery as well as therapeutic agent to combat antibiotic resistant microorganisms. Recently, metallic nanoparticles have been reported to exhibit antimicrobial activity against AMR bacterial strains[6] For example, Nickel and $Ni(OH)_2$ nanoparticles possess antimicrobial activities against multidrug-resistant *K. pneumonia* and *E. coli*[7], copper nanoparticles against *Micrococcus luteus*, *S. aureus, E. coli*, *K. pneumoniae*, *P. aeruginosa*, and few fungal strains [8]. Antimicrobial properties of silver nanoparticles against bacteria, fungi, and viruses are also well-reported in literature[9]. In addition to these, nanoparticles also play role in the textile industry, medicine, water disinfection, and food packaging[10]. Gold nanomaterials are considered to be one of the most suitable nanomaterial for biomedical applications, owing to their inherent biological inertness, well established surface modification procedure and facile and rapid preparation[11]

Biosurfactants produces by microbes, are amphiphilic in nature and have shown antiadhesive and antimicrobial activity[12] [13] [14]. Sophorolipid is a class of glycolipid (biosurfactant), with potential antifungal, antibiofilm, hyphal growth inhibition activity [15]. It has been also shown activity against Gram-Positive bacteria but has not exhibited potent activity against gram-negative bacteria[16]. It is biodegradable, eco-friendly in nature and therefore has been utilized in the greener synthesis of gold nanoparticles (AuNPs-SL). We have demonstrated that sophorolipid capped gold nanoparticles (AuNPs-SL) exhibit potent antimicrobial activity against both Gram-negative and Gram-positive bacteria, with higher efficacy against Gram-negative bacteria[17] However, both AuNPs (uncapped) and sophorolipid (SL) lack antimicrobial activity towards gram negative bacteria when used individually. However, the mechanism of action underlying the antimicrobial effect conferred by AuNPs- SL against Gram negative bacteria remains unclear.

Here, we are reporting the plausible mechanism of action of AuNPs-SL against *V. cholerae*. It has been observed that the treatment of AuNPs-SL initiates a cascade of downstream signaling resulting in over-expression of several genes mitigating the surge in ROS level, regulating ion homeostasis, maintaining membrane integrity, involved in the DNA damage repair inside the cell. The experimental findings of our study suggested that membrane depolarization, ATP depletion, and DNA damage due to AuNPs-SL treatment to the cells, leads to cell death. Thus, the consequent effects of AuNPs-SL may be attributable to the loss of membrane integrity, permeabilization of the cells, and leakage of the cellular content. Thus, our study provides a comprehensive understanding of the plausible mechanism of action of AuNPs-SL against *V. cholerae*.

Materials And Methods

Chemicals and Reagents

Bacterial cultures were grown in Luria Bertini (LB) media purchased from Himedia. Gold (III) chloride hydrate (50790) and Mohr's salt were purchased from Sigma-Aldrich. The dyes $DiBAC_4$ and BACLight™ bacterial membrane potential kit were procured from Invitrogen.

Growth Conditions and Viability

Gram negative *V. cholerae* EL Tor N16961 strain was used in this study. In all the experiments, unless mentioned otherwise, primary inoculums were prepared in LB broth by inoculating an isolated colony of the strain, growth conditions being 37°C, 200 rpm in an orbital shaker overnight. Further, cells in the exponential phase of growth were treated in (OD600 0.2) 10 ml of LB media each time and incubated at 37°C for 3 h followed by PBS wash (pH 7.2) and resuspension in the same buffer. The number of cells was kept constant for further experiments.

Measurement of Reactive Oxygen Species (ROS) generation

To investigate the redox state of the cell, ROS generation was measured using ROS sensitive probe 2,7-dichlorodihydrofluorescein diacetate (H_2DCFDA) fluorescent dye (Sigma, Aldrich). The dye once enters the cell, gets oxidized to form fluorescent product 2',7'-dichlorofluorescein (DCF) [18]. Cells were subjected to different concentrations of AuNPs-SL, washed with PBS thrice, and stained with H_2DCFDA (10 µM) for 1h at 37°C. Quantitative measurement of ROS in the cells after AuNPs-SL treatment was done by flow cytometer (Accuri C_6) using FL1 filter taking 20000 cells in the count. The mean fluorescence intensity (MFI) of 20000 cells was measured by Accuri C_6 using a FL1 filter. The values were normalized to MFI and the data of three independent experiments with ± SD was plotted.

The effect of ROS quenchers were investigated by adding indicated quenchers to the cells during AuNPs-SL-25 treatment for 3 hours. Cells were washed with PBS after centrifugation, stained with H_2DCFDA (10 µM), and measured as mentioned above. Likewise, a growth assay was carried out using a honeycomb plate by adding the indicated compounds to the medium during growth.

Log phase cells were diluted 1000 times and 100 µl of diluted culture was added to honeycomb plate with an equal volume of different ROS quenchers dissolved in LB. The measurement of OD 600 nm was taken at an interval of 1 hour in Bioscreener and a graph was plotted from data obtained.

Effect of DTT on AuNPs-SL stress

ROS measurement due to nanoparticles (AuNPs-SL-25) in the presence and absence of DTT (3 mM) was done using oxidative stress sensitive fluorescent dye H_2DCFDA (10 µM).

AuNPs-SL-25 treated cells were incubated for 3 hours in the presence and absence of DTT. The cells were harvested and stained with $DiOC_2$ for 30 minutes in dark and washed twice with PBS to probe alteration in membrane potential. The fluorescence measurement was done using FL1 filter in Accuri C_6.

LB agar plates with different concentrations of AuNPs-SL nanoparticles (25, 50, and 100 µg/ml) and a combination of AuNPs-SL and DTT (3 mM) were prepared. Primary culture of *V. cholerae* was sub-cultured for 2–3 hours to obtain log-phase cells that were diluted to a ratio of $1:10^2$, $1: 10^4$, $1:10^6$, and 10 µl of each dilution was spotted on these agar plates and incubated overnight (12–14 h) at 37°C. The images of plates were taken and represented.

Membrane Depolarization Assay

After completion of the incubation period of untreated and AuNPs-SL treated were centrifuged at 4000 rpm and the cell pellet is washed with PBS. The cells were resuspended in 10 µM $DiBAC_4$ (1 mM DMSO) and incubated for 30 minutes at 37°C in dark. Further, the cells were washed and resuspended in PBS. Flow cytometric data of 20000 cells was acquired using an FL1 laser of Accuri C_6 Flow Cytometer.

Loss of membrane potential was also analyzed by using dye 3,3'-diethyloxacarbocyanine iodide ($DiOC_2$, BacLight™ Bacterial Membrane potential Kit, Molecular Probes/Invitrogen), a membrane potential sensitive dye. For this, the cells were stained with 2.5 µM of dye for 20 min at 37°C in dark. Thereafter,

cells were washed with PBS, and FACS data was acquired for 10000 cells using an FL1 laser of Accuri C_6 Flow Cytometer.

Real Time Quantitative PCR (RT-qPCR)

To check the expression profile of the selected genes in presence of AuNPs-SL (10 µg/ml) treatment, RT-qPCR was performed. The RNA extraction was done using Trizol reagent method and clean up was done using Qiagen Kit. The RNA was checked for its quality and quantified using Nano-Drop Spectrophotometer. One step SYBER Green Master Mix reaction mixture (Invitrogen) was used to perform the qPCR reaction in a Fast Real-time PCR system (Applied Biosystem) with 200 ng of RNA per reaction. The data of triplicate experiments of biological triplicates was plotted with SD in terms of fold change in expression level.

Measurement of different metal ion concentration upon AuNPs-SL stress

To evaluate the change in the intracellular concentration of different metal ions, log phase cells were grown in the presence of AuNPs-SL (10 µg/ml) for 2–3 hours, harvested, and washed twice with 1X PBS (pH 7.2). Metal ion concentration within the cell pellets (20 mg) was determined by using an ICP-MS machine at (Punjab Biotechnology Incubator, Mohali, India). The cell pellet was digested with 5 ml of concentrated nitric acid and 0.5 ml hydrogen peroxide (30%). The final volume of the Digested sample was adjusted to 50 ml with deionized water and the sample was analyzed by ICP-MS. The amount of ion present was reported in mg/kg of cell pellet.

Effect of Iron supplementation using Mohr's salt under AuNPs-SL stress

Log phase cells were diluted 1000 fold and different combinations were prepared in LB broth (100 µl) and different preparation was mixed to 100 µl diluted culture and added to 100 well honeycomb plates. The growth assay was performed in Bioscreener at 37°C for 16 hours and the OD600 was measured at every 1 hour of incubation.

LB agar plate with different concentrations of AuNPs-SL (25 µg/ml), Mohr's salt (1.5 mM), and a combination of the two was prepared. *V. cholerae* cells at log phase were diluted to a ratio of $1:10^2$, $1:10^4$, $1:10^6$, and 10 µl of each was spotted on agar plates followed by overnight incubation at 37°C. The representative images of plates are given in Fig. 5C.

Relative ATP measurement

Relative ATP estimation was done using ATP Bioluminescence Assay Kit CLS II (Roche) following the manufacturer's recommended protocol. Briefly, the cells were harvested and washed with chilled PBS. To extract ATP, the cells were incubated in ATP extraction buffer (100 mM Tris-HCl, pH 7.75 and 4 mM EDTA, pH 8.0) at 100°C for 2 minutes, followed by separation of cell-free supernatant by centrifugation for 5

minutes at 1000 g. 50 µl each of sample supernatant and luciferase reagents was added to wells in Black 96 well microplate with gentle mixing and the luminescence was measured using a luminometer. The relative light units (RLU) were recorded and normalized, against per milligram of protein. The normalized RLU's were plotted with SD.

TUNEL (TdT-mediated dUTP-X nick end labeling) assay

To check if the nanoparticles are promoting apoptotic-like cell death in *V. cholerae*, a TUNEL assay was performed following kit protocol. Briefly, cells were harvested after treatment with AuNPs-SL (25 µg/ml) and nalidixic acid (5 µg/ml) for 3 hours. Cells were then washed with PBS (pH 7.2), fixed with 2% formaldehyde for (15 min on ice), and treated post-fixation with 70% ethanol. The fixed cells were permeabilized with permeabilization buffer (0.1% Triton X-100 and 0.1% sodium citrate) while kept on ice for 2 min. After washing the cells were resuspended in 50 µl of the solution containing enzyme (terminal deoxynucleotidyl transferase, TdT) and reaction mixture in the ratio of 1:9. After one hour of incubation at 37°C, the cells were washed again and collected after final resuspension in PBS. The FACS data of 20000 cells were acquired using an FL1 laser of Accuri C_6 FACS machine and the Mean fluorescence values of three independent experiments have been plotted with SD.

Apoptosis Assay

To check the apoptotic like cell death in i.e., *V. cholerae* (prokaryotes), we performed annexin affinity assay. In brief, the cells were treated with AuNPs-SL (taking untreated as control) were washed twice with PBS buffer, and stained with Annexin V allophycocyanin conjugate (5 µg/ml) for 20 min. Cells were washed with PBS to remove the unbound form of stain and determined signal from 20000 cells using FL4 filter FACS.

Cell morphology analysis using TEM

To determine the change in the ultrastructure of *V. cholerae* cells induced by the AuNPs-SL treatment, sample preparation, and Transmission Electron Microscopy (TEM) micrograph were taken as followed by [19] with slight modifications. In brief, both treated (AuNPs-SL 25 µg/ml for 3 h) and untreated cells were washed with PBS twice fixed with modified Karnovsky's fixative containing 2% (V/V) glutaraldehyde and 2% (V/V) paraformaldehyde in 0.1 M sodium cacodylate buffer (pH 7.2) at 4°C for 2 h[20]. This was followed by washing with PBS and post-fixation treatment with 0.2 M sodium cacodylate buffer and osmium tetroxide (OsO_4) (200 µl of 2% (W/V)) at 4°C for 90 minutes. The sample was washed thrice with 0.1 M sodium cacodylate buffer and resuspended in the same buffer containing 2% agarose. A thin section was cut by microtome followed by its gradual dehydration with acetone solution (once in 30, 50, 70, and 90% and twice in 100). Finally, the sections were examined under TEM in JEOL-2100.

Measurement of cellular contents (protein, DNA) leaked due to AuNPs-SL treatment

To determine the leakage of cellular content (protein and DNA), the cells were treated with different concentrations of nanoparticles (AuNPs-SL; 25 and 50 µg/ml) followed by a Bradford assay and

Nanodrop measurement to quantify the protein and DNA content of the samples, respectively.

For measurement of protein, 1 ml of cell sample (treated and untreated) was withdrawn after 2 h incubation of AuNPs-SL treatment. The supernatant of cells was used for protein quantification by the Bradford method (Bradford, 1976a). For measurement of DNA, untreated and treated cells were harvested and DNA was extracted from the supernatant as per manufacturer instruction (ZR Fungal/Bacterial DNA Kit™ Catalog No. D6005). DNA quantification was done by a Nanodrop spectrometer.

Statistical analysis

The data from three independent experiments are represented as the mean ± standard deviation of the mean. Either paired or unpaired *t*-test analysis (mentioned in the graph) was performed using GraphPad Prism 6 software for analysis.

Results And Discussion

AuNPs-SL induces ROS production in V. Cholerae

Nanoparticle mediated killing of bacteria is known to be associated with ROS generation, leading to alteration of membrane structure and function, causing cellular stress and cell death[21]. Therefore, ROS production within the AuNPs-SL treated *V. cholerae* cells was measured using oxidative stress sensitive probe H_2DCFDA. AuNPs-SL treated (treatment range 10–25 µg/ml) cells exhibited dose dependent increase in ROS production ranging from 2.5 to 20 fold (Fig. 1A). However, different ROS scavengers showed varied ROS quenching potential (Fig. 1B). The magnitude of ROS scavenging capacity was highest with N-acetyl-L-cysteine (NAC) followed by tiron (Tr), ascorbate (all ~ 5–6 fold), thiourea (TU), and sodium pyruvate (SP) (both ~ 3 fold). The Tr, TU, and SP scavenge $^{\bullet}O_2$, H_2O_2, and $^{\bullet}OH$ radicals, respectively. These results strongly suggest that the treatment of AuNPs-SL leads to the generation of at least three different ROS species. Nevertheless, the presence of different scavenging agents in the growth medium could rescue the growth of the *V. cholerae* treated with AuNPs-SL (Fig. 1C). However, the effect of ascorbate and SP was not sufficient for the rescue of growth of the cells from the effect of ROS.

NAC mediated scavenging of free radicals is mediated by increased intracellular glutathione level[22]. However, the reduction of ROS concentration by NAC is exhibited through a thiol-disulphide[23] exchange which may be responsible for this function. Although ascorbate and SP exhibit significant ROS scavenging effect, neither of the compounds were able to rescue the growth of the dying cells. (Fig. 1B and 1C) Similar phenomena were observed with cells treated with silver nanoparticles[24]. This result also infers that the nanoparticles also interact with the respiratory enzymes the function of which are rescues after NAC supplement.

Effect of DTT on AuNPs-SL treated cells

DTT, a strong reducing agent, has been reported to rescue cells from oxidative stress and restore their growth[25]. The effect of DTT on ROS generation in AuNPs-SL treated *V. cholerae* was checked by adding the compound in the culture medium. The treatment with DTT rescued the cells from ROS mediated oxidative stress generated in presence of AuNPs-SL (supplementary Fig. 1A). However, the presence of DTT could not stop the alteration in membrane potential due to AuNPs-SL treatment (supplementary Fig. 1B). In contradiction to the observation made by Wang et al., 2017.,[26], in our study, the addition of salicylate with DTT was unable to recuperate the membrane potential of the AuNPs-SL treated cells. However, the exact mechanism leading to this effect remains obscure. When the cells were cultured in LB agar plate containing AuNPs-SL (25–100 µg/ml), no growth was observed. However, the growth of the cells was rescued when treated cells were supplemented with DTT (Supplementary Fig. 1C). The possibility of structural alteration or aggregation of AuNPs-SL in presence of DTT was ruled out by incubating nanoparticles with DTT for a certain time interval. No significant alteration in the UV spectra was observed in nanoparticles incubated with DTT (Supplementary Fig. 1D).

Treatment of V. cholerae **with AuNPs-SL leads to membrane depolarization**

Oxidative stress leads to the alteration of membrane potential. The alteration of membrane potential in *V. cholerae* was measured in presence of various concentrations of AuNPs-SL using two different dyes, DiBAC4 and DiOC2. DiBAC4 is an anionic lipophilic bis-oxonol dye. During membrane depolarization, as the membrane potential shifts from negative towards positive, the concentration of the dye entering the cells also increases (*i.e.*, the higher the membrane is depolarized, more is the oxonol fluorescence intensity). In our experimental setup, when the *V. cholerae* cells were treated with 10 and 25 µg/ml AuNPs-SL, membrane depolarization was increased by 13% and 16%, respectively (Fig. 2A & B). In addition, the *V. cholerae* cells treated with AuNPs-SL exhibited concentration dependent change in fluorescence intensity of $DiOC_2$ (Fig. 2C & D), where, the change in fluorescence intensity of $DiOC_2$ is directly proportional to loss of membrane potential of the cells [27] .

Effect of AuNPs-SL on the stress response gene of the V. cholerae

V. cholerae treated with AuNPs-SL undergo oxidative stress due to ROS generation within the cell. ROSs, including $\bullet O_2$, H_2O_2, and •OH are highly toxic and cause damage to the cells. Microorganisms respond to the higher level of cellular ROS concentration by triggering the multigenic response. Therefore, the expression profile of several selected genes was checked in the AuNPs-SL treated cells using qRT-PCR (Fig. 3). The genes used in the study and their respective primers are enlisted in Table 1.

Table 1
List of primers used in the RT-qPCR

Primers		Sequence 5′-3′	Tm (°C)	Amplified product size (bp)
dps	F	TGCACAGCTTTAGCGGTTAC	55.96	119
	R	TTGTTGGTGGAGCAGAATGC	56.11	
oxyR	F	GCACTTATTGTTGCGCGAAG	55.95	123
	R	CCCACCACATAGCTCTCCAT	55.86	
grx	F	TACCGCTTATGCAACGCAAA	55.95	110
	R	TTCCAGCCGATCATCAAACG	55.74	
gsp	F	GCTCTCTCAAGCGGAGTTTG	56.06	121
	R	TTCCGCCAGTGAGAAGAAGT	55.98	
luxO	F	ACTGCGGGTCACAGTGAATA	56.06	135
	R	GAGTCAATGGTGCGGTACAC	56.05	
katE,	F	GGTGATTAAGGCCGCACAAA	56.19	112
	R	AGCCATTTGCTGCCAATCTT	55.74	
ompU	F	CGGTGACAAAGCAGGTTCAA	56.07	120
	R	CGTACGCGAGAGTTGTCTTG	56.23	
recA	F	GGGCGTGAATATCGATGAGC	56.07	102
	R	ATGACATCCACAGCACCAGA	56.02	
sodA	F	GTGAACACCTTTGGCTCTGG	56.13	106
	R	CGGCAACCACATCCATCAAT	55.96	
soxR	F	GAAGGTCTCAGCGTTGCATT	55.94	140
	R	AGGTCAGTCCGACCATTTGT	55.95	
fur	F	ACAGCCAGAGTGCCAACATA	56.32	130
	R	ACGAGTCACGATACCAGCAT	55.96	
luxR	F	GATCCAAACCGCTCAGCATT	55.98	139
	R	TGGCGTTACGCAAGTGATTT	55.82	

The *sodA* being a part of the cellular defense system during oxidative stress, is involved in the conversion of superoxide anion ($O_2^{\bullet-}$) to O_2 and H_2O_2 that ultimately gets reduced to H_2O by catalase [28]. We have

observed ~ 5 fold increase in *sodA* expression in AuNPs-SL treated cells. The expression of *sodA* is controlled by *soxSR* regulon, which is also involved in the regulation of expression of more than 40 other genes. Excess superoxide radicals trigger the activation of *soxSR* regulons like *soxR*. The oxidized form of *soxR* acts as a transcription activator of *sodA* [29].

We have also observed ~ 4 fold upregulation in the expression of *oxyR* (a ROS-sensing transcriptional regulator). The *oxyR* is a master regulator mediating cellular response to the higher concentration of H_2O_2 within the cells. The *oxyR* mediated regulation of *k*at*E* is well studied in Gram (−ve) bacteria [30] [31].. An increase in intracellular H_2O_2 level triggers the expression of *oxyR* regulon including catalase. Therefore, in AuNPs-SL treated cells, the expression level of hydroxyl peroxidase (*katE*) was also elevated; probably, to mitigate the oxidative damage caused by the H_2O_2.

The *oxyR* is an H_2O_2 scavenging LysR family protein, regulated with an N-terminal helix-turn-helix DNA binding domain. In presence of H_2O_2 *oxyR* changes to rearrange its secondary structure by forming an intramolecular disulfide bond resulting in the oxidized form of *oxyR*, which binds to its target site to execute its regulatory function. It can alter the expression of several genes including the H_2O_2 detoxification gene (*katE*), genes for FeS-centre repair, iron transport and sequestration (*fur*), and Mn import.

Further, the DNA binding protein (*dps*) has shown an increased expression of ~ 2.5 fold due to AuNPs-SL treatment to the cells. The expression of *dps*, is known to be involved in ROS resistance during the exponential growth phase and is regulated by *oxyR*. Nonspecific DNA binding of *dps* protects DNA against damage from ROS and the physical association of DNA with the toxic combination of Fe_2 and H_2O_2. In *E. coli*, *dps* is also involved in tolerance to acid stress Fe[32] and Cu toxicity [33] [34] The increased expression of *dps* is involved with ameliorating the ROS damage in *oxyR* dependent manner[30] [35]. The global regulator of iron homeostasis, ferric uptake regulator (*fur*), mediates the oxidative stress defense mechanism [36] in *V. cholerae*. We have observed two fold upregulation in *fur* expression, indicating perturbation in the iron uptake and homeostasis within the AuNPs-SL treated cells. An overexpression of 5–6 fold of *grx* was also observed within the treated cells.

The o*mpU* plays a critical role during the adhesion of *V. cholerae* to the host[37], which was down regulated in the AuNPs-SL treated cells. In the case of bacteria, outer membrane proteins play an important role in adaptation to the external environment. In *Vibrio sp.*, the *OmpU* is a major porin involved in the adhesion/colonization of the bacteria. It helps to confer resistance to the microbes against antimicrobial peptides (AMPs) and bile toxicity in the host. Though, under iron limited condition, downregulation of the expression of the *omp*s', as the receptor of siderophore complex and heme-compound transporter have been observed in *V. cholerae*[38], down regulation of *ompU* under AuNPs-SL treated condition suggested alteration in iron transportation within the cells. Moreover, down regulation of *ompU* indicates impaired cell evasion and biofilm formation.

The *luxO* regulates multi-signal transduction system, was upregulated by seven folds indicating an increase in colonization tendency during oxidative stress in *V. cholerae* upon AuNPs-SL treatment. In *V. cholerae*, the *gsp* plays an important role in the secretion of secretory proteins, and proper outer membrane assembly (general secretion pathway), is required for the export of several proteins like chitin, cholera toxin, and protease [39] [40]. It also aids in the survival of *V. cholerae* under different stress conditions by facilitating biofilm formation, pathogenesis, the release of enterotoxin, biofilm dispersal, and membrane biogenesis[39]. AuNPs-SL treatment upregulated expression of *gsp* by three folds. Likewise, two-fold upregulation of *recA* was observed indicating ROS mediated SOS response in bacterial cells under stress conditions. The up regulation of the ROS responsive genes indicated AuNPs-SL treatment leads to the perturbation of several cellular and physiological functions and leading to the killing of *V. cholerae* cells.

AuNPs-SL treatment of V. cholerae **alters metal ion concentration within the cells**

For the maintenance of membrane potential, the cell requires the movement of ions across the cytoplasmic membrane. Consequent to the alteration of membrane potential due to AuNPs-SL treatment and subsequent gene expression profile prompted us to find the ion concentration within the *V. cholerae* cells. Sodium and potassium are the major regulatory ions for the maintenance of the membrane potential. Therefore, the concentration of major ions related to membrane potential and cellular stress physiology was checked by using ICP-MS. Treatment of *V. cholerae* with AuNPs-SL led to the increase in the K+, Na + and Fe^{2+} concentration inside the cells, whereas Ca^{2+} concentration remained unaltered (Table 2). Thus, the alteration of K + and Na + concentration supported the change in membrane potential and the alteration of Fe^{2+} concentration indicated disruption in iron homeostasis and related physiology within the AuNPs-SL treated cells.

Table 2
Ion concentration measurement under nanoparticles stress

Ions concentration (unit: mg/kg)	**Control**	**AuNPs-SL-10**
Iron	146	229
Sodium	2058	4076
Potassium	2655	4434
Calcium	1591	1583

Supplementation of Fe^{2+} using Mohr's salt rescue V. cholerae **from AuNPs-SL stress**

Iron is an essential micronutrient for the growth and metabolism of microorganisms, plays important role in ROS generation via Fenton reaction [41], and works as a cofactor for various enzymes viz. [Fe–S]-containing ferredoxins, heme-containing cytochromes, fumarases, etc[42]. In bacterial cells, iron uptake

and storage are critically controlled and regulated by the cellular physiology and homeostatic mechanism. Since, the iron concentration increased within the cells due to AuNPs-SL treatment, we presumed that iron was not available for physiological functions. Therefore, the effect of external iron supplementation was checked in the *V. cholerae* in presence of AuNPs-SL. Growth kinetic studies revealed that the growth was rescued after iron supplementation to the growth medium via Mohr's salt (Fig. 4A). In addition to that, Mohr's salt supplementation significantly decreased the ROS production within the treated cells (Fig. 4B). Further, the growth of *V. cholerae* in Mohr's salt supplemented agar plate indicated recovery of the cells from ROS stress. The supplementation of Mohr's salt may have helped the cells in repairing the impairment of Fe-S cluster assemblies, an integral part of the electron transport chain (ETC), the impairment of which leads to the ROS generation[43]. Therefore, the cell regained their growth potential and viability.

AuNPs-SL treatment decrease ATP production and creates DNA damage in V. cholerae

The aforementioned impairment of iron clusters related to ETC and alteration in membrane potential in AuNPs-SL treated *V. cholerae*, prompted us to investigate the cellular ATP level. The process of ATP production requires maintenance of membrane potential and membrane integrity as well as proper function of the ETC. Using luciferase based ATP bioluminescence assay, we observed ~ 50% reduction in ATP synthesis in AuNPs-SL treated cells. However, no dose dependent decrease in ATP synthesis was observed in the treated range (10 and 25 µg/mL) of AuNPs-SL (Fig. 5A).

An increase in ROS level within the cells is known to damage DNA by creating lesions in bases, sugar, DNA protein cross links within the single and double strand bases of DNA. Overexpression of *dps* and *recA*, DNA protecting and damage repair elements, indicates considerable DNA damage within the AuNPs-SL treated cells. The TUNEL assay used for the estimation of DNA fragmentation measures fluorescence from the free 3'-OH of the damaged DNA, synthesized from fluorescein labeled dUTP by exogenously supplied terminal deoxynucleotidyl transferase. The incorporation of labeled dUTP increases fluorescence inside the cells. When the cells were treated with AuNPs-SL, we observed 20 fold increase in the fluorescence intensity (Fig. 5B) indicating severe DNA damage and fragmentation within cells in AuNPs-SL treated condition.

AuNPs-SL treatment leads to apoptosis in V. cholerae

DNA fragmentation is a hallmark of the initiation of programmed cell death or apoptosis. Therefore, we checked for the initiation of cellular apoptosis within the *V. cholerae* treated with AuNPs-SL by using Annexin V allophycocyanin conjugate. Figure 6A shows a significant shift in a population showing annexin affinity upon AuNPs-SL treatment. Around 5 fold increases in the fluorescence intensity of Annexin V have been observed within the treated cells (25 µg/mL of AuNPs-SL treatment); however, the effect of a lesser amount of AuNPs-SL (10 µg/mL) was not significant (Fig. 6B). Nevertheless, this result indicated the presence of a significant amount of apoptotic cellular population upon AuNPs-SL treatment.

AuNPs-SL treatment causes cell wall damage and membrane leakage in V. cholerae

The bactericidal activity of AuNPs-SL against *V. cholerae* suggests the interaction of the AuNPs-SL with the cell membrane. Therefore, the effect of the AuNPs-SL was checked on the outer surface and cell membrane of *V. cholerae* by TEM. Extensive damage of the outer surface with ruptured membrane was observed in the AuNPs-SL treated cells compared to the controlled one (Fig. 7A(i) and 7A(ii)). Damaged cell wall and membrane led to the outflow of cellular protein and DNA in the surrounding environment; therefore, we measured the amount of released protein and DNA from the cell. There was a significantly higher amount of release of cellular protein from the AuNPs-SL treated cells. We also observed a concentration-dependent release of protein and DNA with an increasing dose of AuNPs-SL (Fig. 7B and 7C). Treatment with 25 and 50 µg/ml of AuNPs-SL treatment of *V. cholerae*, resulted in a twofold and fourfold increase in DNA leakage respectively.

Conclusion

This study mechanistically explains the antimicrobial effect of AuNPs-SL as shown in Fig. 8. AuNPs-SL exerts its effect by interacting with the bacterial membrane and causing physical damage to the membrane. The perturbed membrane has other physiological consequences e.g. membrane potential alterations, PMF disturbances, leakage of intracellular content, etc. The altered membrane potential and PMF deplete the ATP level in the cell. The membrane perturbations also lead to the accumulation of AuNPs-SL in the cells. Intracellular accumulation of AuNPs-SL generates ROS which further causes oxidative stress, apoptosis, oxidative damage to the proteins, and metal ion disturbances in the cells. To mitigate these physiological assaults, the treated cells alters the expression of the genes of respective pathways. In summary, membrane damage and ROS formation are the primary causes of AuNPs-SL mediated killing of *V. cholerae*. The killing effect to the bacterial cell is brought about at a reasonably low concentration (MIC). Therefore, the AuNPs-SL has the potential to serve as an alternative therapy for the removal of water-borne microbial pathogens. Nevertheless, the understanding of the molecular mechanisms associated with the killing of *V. cholera* by AuNPs-SL provides us with an opportunity to understand its feasibility as an alternate antimicrobial agent in the future.

List Of Symbols

AMR
Antimicrobial resistance
ATP
Adenosine triphosphate
AuNPs-SL
Sophorolipid-capped gold nanoparticles
DMSO
Dimethylsulfoxide
DTT

Dithiothreitol
ETC
Electron Transport Chain
LB
Luria Bertani
µg/ml
microgram
µM
micromolar
mg
Milligram
MIC
Minimal Inhibitory Concentration
ml
Millilitre
PBS
Phosphate Buffer Saline
PMF
Proton Motive Force
ROS
Reactive oxygen species
TEM
Transmission Electron Microscopy

Declarations

Ethics approval and consent to participate

Not applicable.

Consent for publication

Not applicable.

Data availability

All data generated or analysed during this study are included in this article.

Competing interests

The authors declare that they have no competing interests.

Funding

The authors gratefully acknowledge the financial support provided by the Council of Scientific and Industrial Research, Govt. of India for carrying out the research.

Author contributions

SS contributed to the conception of the work, design of the experiments, investigation and result analysis, drafting manuscript; VK contributed to the design of the work, investigation and result analysis, drafting manuscript; DD contributed in the conception, interpretation of data, supervision and correcting manuscript; MSB contributed to the conception, investigation, interpretation of data, supervision and drafting the manuscript, administration and submission; All authors read and approved the final manuscript.

Acknowledgments

The authors gratefully acknowledge the financial support provided by the Council of Scientific and Industrial Research, Govt. of India for carrying out the research. SS and VK acknowledge the financial support for providing research fellowship by Indian Council for Medical Research (ICMR), Govt. of India whereas AJ acknowledges University Grant Commission (UGC) Govt. of India.

Author's information

[1]Biochemical Engineering Research and Process Development Centre (BERPDC), CSIR-Institute of Microbial Technology (IMTECH), Sector-39A, Chandigarh 160036, India.

[2]MolecularMicrobiology laboratory, CSIR-Institute of Microbial Technology (IMTECH), Sector-39A, Chandigarh 160036, India.

References

1. Gugnani HC. Some emerging food and water borne pathogens. J Commun Dis. 1999;31:65–72.
2. Faruque SM, Chowdhury N, Kamruzzaman M, Dziejman M, Rahman MH, Sack DA, et al. Genetic diversity and virulence potential of environmental Vibrio cholerae population in a cholera-endemic area. Proc Natl Acad Sci U S A. 2004;101:2123–8.
3. Charles RC file:///C:/Users/Dell/Desktop/shrist. mam papers/080048. pd., Ryan ET. Cholera in the 21st century. Curr. Opin. Infect. Dis. 2011. p. 472–7.
4. D. S, M.M. K, W.A. K, S. A, M.A. S, M.L. B. Single-dose azithromycin for the treatment of cholera in adults. N. Engl. J. Med. 2006. p. 2452–62.
5. Llor C, Bjerrum L. Antimicrobial resistance: Risk associated with antibiotic overuse and initiatives to reduce the problem. Ther Adv Drug Saf. 2014;5:229–41.
6. Lee NY, Ko WC, Hsueh PR. Nanoparticles in the treatment of infections caused by multidrug-resistant organisms. Front Pharmacol. 2019;10:1–10.

7. Mirhosseini M, Kheiri Hafshejani B, Dashtestani F, Hakimian F, Haghirosadat BF. Antibacterial activity of nickel and nickel hydroxide nanoparticles against multidrug resistance K. pneumonia and E. coli isolated urinary tract. Nanomedicine J. 2018;5:19–26.
8. Ramyadevi J, Jeyasubramanian K, Marikani A, Rajakumar G, Rahuman AA. Synthesis and antimicrobial activity of copper nanoparticles. Mater Lett. 2012;71:114–6.
9. Salleh A, Naomi R, Utami ND, Mohammad AW, Mahmoudi E, Mustafa N, et al. The potential of silver nanoparticles for antiviral and antibacterial applications: A mechanism of action. Nanomaterials. 2020;10:1–20.
10. Makvandi P, Iftekhar S, Pizzetti F, Zarepour A, Zare EN, Ashrafizadeh M, et al. Functionalization of polymers and nanomaterials for water treatment, food packaging, textile and biomedical applications: a review. Environ Chem Lett. Springer International Publishing; 2021;19:583–611.
11. Bansal SA, Kumar V, Karimi J, Singh AP, Kumar S. Role of gold nanoparticles in advanced biomedical applications. Nanoscale Adv. Royal Society of Chemistry; 2020;2:3764–87.
12. Janek T, Łukaszewicz M, Krasowska A. Antiadhesive activity of the biosurfactant pseudofactin II secreted by the Arctic bacterium Pseudomonas fluorescens BD5. BMC Microbiol. 2012;12.
13. Luna JM, Rufino RD, Sarubbo LA, Rodrigues LRM, Teixeira JAC, De Campos-Takaki GM. Evaluation antimicrobial and antiadhesive properties of the biosurfactant Lunasan produced by Candida sphaerica UCP 0995. Curr Microbiol. 2011;62:1527–34.
14. Rivardo F, Turner RJ, Allegrone G, Ceri H, Martinotti MG. Anti-adhesion activity of two biosurfactants produced by Bacillus spp. prevents biofilm formation of human bacterial pathogens. Appl Microbiol Biotechnol. 2009;83:541–53.
15. Haque F, Alfatah M, Ganesan K, Bhattacharyya MS. Inhibitory Effect of Sophorolipid on Candida albicans Biofilm Formation and Hyphal Growth. Sci Rep. Nature Publishing Group; 2016;6.
16. Shah V, Badia D, Ratsep P. Sophorolipids having enhanced antibacterial activity [1]. Antimicrob Agents Chemother. 2007;51:397–400.
17. Shikha S, Chaudhuri SR, Bhattacharyya MS. Facile One Pot Greener Synthesis of Sophorolipid Capped Gold Nanoparticles and its Antimicrobial Activity having Special Efficacy Against Gram Negative Vibrio cholerae. Sci Rep. 2020;10.
18. Eruslanov E, Kusmartsev S. Identification of ROS using oxidized DCFDA and flow-cytometry. Methods Mol Biol. 2010;594:57–72.
19. Woo KJ, Hye CK, Ki WK, Shin S, So HK, Yong HP. Antibacterial activity and mechanism of action of the silver ion in Staphylococcus aureus and Escherichia coli. Appl Environ Microbiol. 2008;74:2171–8.
20. Karnovsky MJ. A formaldehyde-glutaraldehyde fixative of high osmolality for use in electron microscopy. J Cell Biol. 1965;27:137–8.
21. Raghupathi KR, Koodali RT, Manna AC. Size-dependent bacterial growth inhibition and mechanism of antibacterial activity of zinc oxide nanoparticles. Langmuir. 2011;27:4020–8.

22. Ates B, Abraham L, Ercal N. Antioxidant and free radical scavenging properties of N-acetylcysteine amide (NACA) and comparison with N-acetylcysteine (NAC). Free Radic Res. 2008;42:372–7.
23. Sun SY. N-acetylcysteine, reactive oxygen species and beyond. Cancer Biol. Ther. 2010.
24. Kim JS, Kuk E, Yu KN, Kim JH, Park SJ, Lee HJ, et al. Antimicrobial effects of silver nanoparticles. Nanomedicine Nanotechnology, Biol Med. 2007;3:95–101.
25. Pani G, Colavitti R, Bedogni B, Anzevino R, Borrello S, Galeotti T. A redox signaling mechanism for density-dependent inhibition of cell growth. J Biol Chem. 2000;275:38891–9.
26. Wang T, El Meouche I, Dunlop MJ. Bacterial persistence induced by salicylate via reactive oxygen species. Sci Rep. 2017;7.
27. Novo DJ, Perlmutter NG, Hunt RH, Shapiro HM. Multiparameter flow cytometric analysis of antibiotic effects on membrane potential, membrane permeability, and bacterial counts of Staphylococcus aureus and Micrococcus luteus. Antimicrob Agents Chemother. 2000;44:827–34.
28. Niederhoffer EC, Naranjo CM, Bradley KL, Fee JA. Control of Escherichia coli superoxide dismutase (sodA and sodB) genes by the ferric uptake regulation (fur) locus. J Bacteriol. 1990;172:1930–8.
29. Vattanaviboon P, Panmanee W, Mongkolsuk S. Induction of peroxide and superoxide protective enzymes and physiological cross-protection against peroxide killing by a superoxide generator in Vibrio harveyi. FEMS Microbiol Lett. 2003;221:89–95.
30. Jiang Y, Dong Y, Luo Q, Li N, Wu G, Gao H. Protection from oxidative stress relies mainly on derepression of OxyR-dependent KatB and Dps in Shewanella oneidensis. J Bacteriol. 2014;196:445–58.
31. Li N, Luo Q, Jiang Y, Wu G, Gao H. Managing oxidative stresses in S hewanella oneidensis: intertwined roles of the OxyR and OhrR regulons. Environ Microbiol. 2014;16:1821–34.
32. Jeong KC, Hung KF, Baumler DJ, Byrd JJ, Kaspar CW. Acid stress damage of DNA is prevented by Dps binding in Escherichia coli O157:H7. BMC Microbiol. 2008;8:1–13.
33. Thieme D, Grass G. The Dps protein of Escherichia coli is involved in copper homeostasis. Microbiol Res. Elsevier; 2010;165:108–15.
34. Zhao G, Ceci P, Ilari A, Giangiacomo L, Laue TM, Chiancone E, et al. Iron and hydrogen peroxide detoxification properties of DNA-binding protein from starved cells. A ferritin-like DNA-binding protein of Escherichia coli. J Biol Chem. Â© 2002 ASBMB. Currently published by Elsevier Inc; originally published by American Society for Biochemistry and Molecular Biology.; 2002;277:27689–96.
35. Ochsner UA, Vasil ML, Alsabbagh E, Parvatiyar K, Hassett DJ. Role of the Pseudomonas aeruginosa oxyR-recG operon in oxidative stress defense and DNA repair: OxyR-dependent regulation of katB-ankB, ahpB, and ahpC-ahpF. J Bacteriol. 2000;182:4533–44.
36. da Silva Neto BR, de Fátima da Silva J, Mendes-Giannini MJS, Lenzi HL, de Almeida Soares CM, Pereira M. The malate synthase of Paracoccidioides brasiliensis is a linked surface protein that behaves as an anchorless adhesin. BMC Microbiol. 2009;9:272.

37. Sperandio V, Giron JA, Silveira WD, Kaper JB. The OmpU outer membrane protein, a potential adherence factor of Vibrio cholerae. Infect Immun. 1995;63:4433–8.
38. Lv T, Dai F, Zhuang Q, Zhao X, Shao Y, Guo M, et al. Outer membrane protein OmpU is related to iron balance in Vibrio alginolyticus. Microbiol Res. Elsevier; 2020;230:126350.
39. Hirst TR, Sanchez J, Kaper JB, Hardy SJ, Holmgren J. Mechanism of toxin secretion by Vibrio cholerae investigated in strains harboring plasmids that encode heat-labile enterotoxins of Escherichia coli. Proc Natl Acad Sci U S A. 1984;81:7752–6.
40. Sandkvist M, Morales V, Bagdasarian M. A protein required for secretion of cholera toxin through the outer membrane of Vibrio cholerae. Gene. 1993;123:81–6.
41. Andrews SC, Robinson AK, Rodríguez-Quiñones F. Bacterial iron homeostasis. FEMS Microbiol. Rev. 2003. p. 215–37.
42. Beinert H, Holm RH, Münck E. Iron-sulfur clusters: Nature's modular, multipurpose structures. Science (80-). 1997;277:653–9.
43. Dixon SJ, Stockwell BR. The role of iron and reactive oxygen species in cell death. Nat. Chem. Biol. 2014. p. 9–17.

Figures

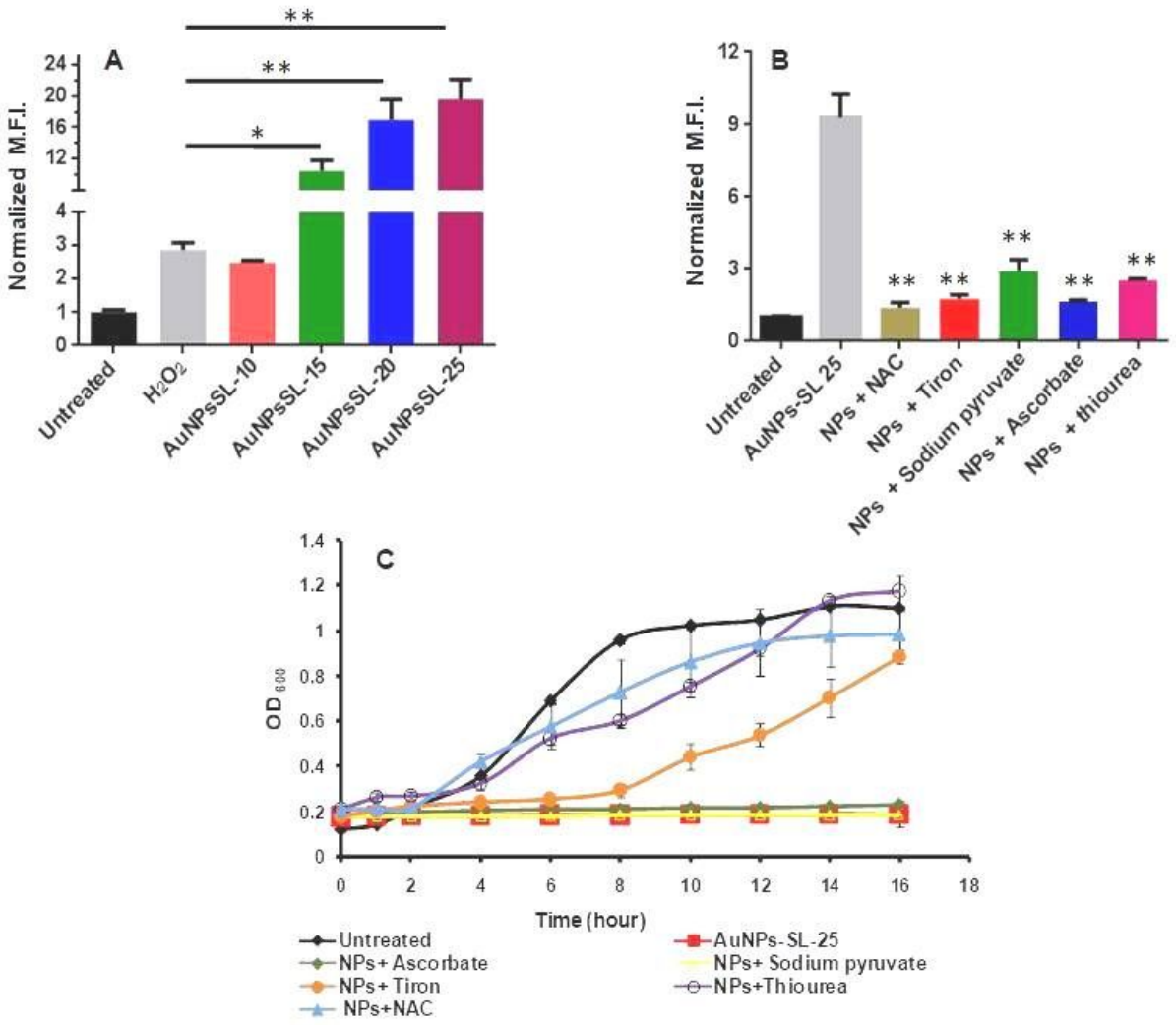

Figure 1

Reactive oxygen species formation in the presence of AuNPs-SL nanoparticles. A. Flow cytometry analysis of ROS measurement in *V. cholerae* exposed to different concentrations of AuNPs-SL (10,15, 20 and 25), **B.** ROS measurement in the presence of AuNPs-SL-25and ROS scavengers (NAC, Tiron, Sodium pyruvate, Ascorbate, Thiourea), **C.** Growth assay of *V. cholerae* in the presence of AuNPs-SL-25 and ROS scavengers (NAC, Tiron, Sodium pyruvate, Ascorbate, Thiourea). (n=3 ± SD). Data is analyzed through paired *t*-test, **P*< 0.01.

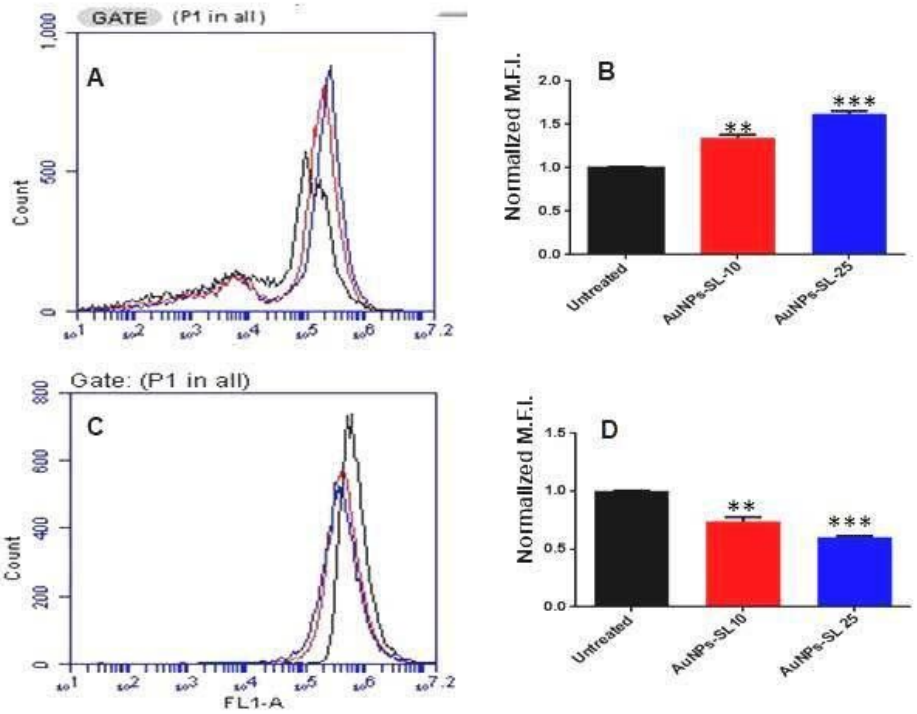

Figure 2

Membrane potential measurement in *V. cholerae* treated with AuNPs-SL. (A &B) Flow cytometric analysis of the membrane potential using DiBAC4. A concentration-dependent increase in Mean Fluorescence Intensity (MFI) indicating plasma membrane depolarization. **(C &D)** Membrane potential analysis using DiOC2. A concentration-dependent decrease in Mean Fluorescence Intensity (MFI) indicating plasma membrane depolarization. (n=3 ± SD). The data analyzed using paired *t*-test, **P*-value < 0.01.

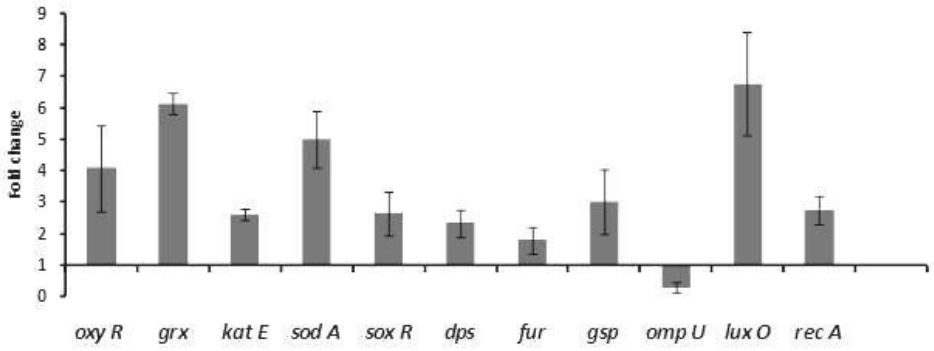

Figure 3

Gene expression in AuNPs-SL nanoparticles treatment. RT-qPCR of selected genes in the presence of AuNPs-SL-25. The bar diagrams represent the fold change of genes in presence of nanoparticles as compared to control. The data of biological duplicates has been plotted with ± SD.

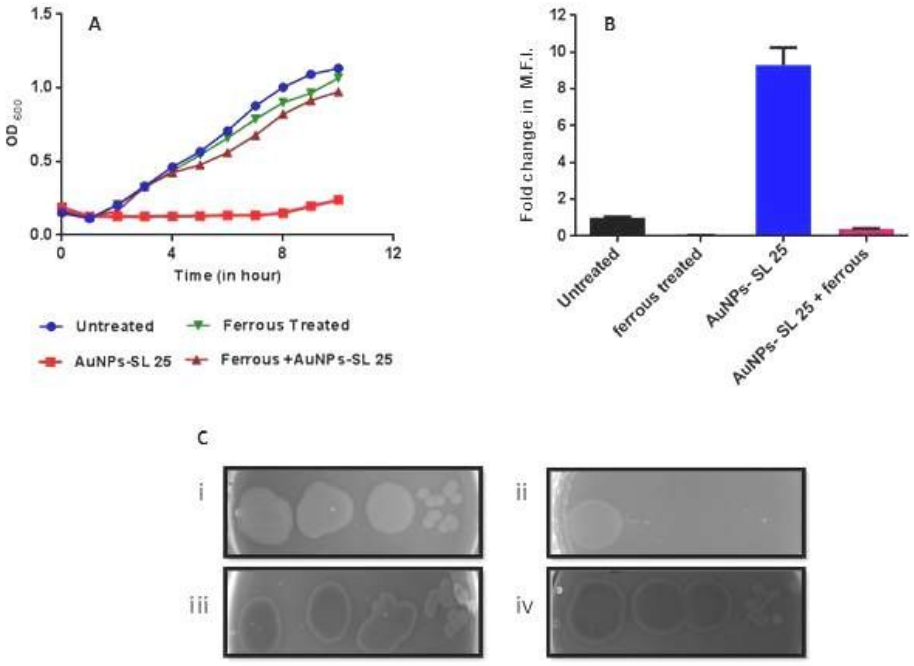

Figure 4

Supplementation of Iron (Mohr's salt) rescues the growth inhibitory effect of AuNPs-SL nanoparticles. A. Growth assay, **B.** ROS measurement, **C.** Spot assay in the presence AuNPs-SL-25 and Iron. **P* value<0.01 calculated through paired t-test.

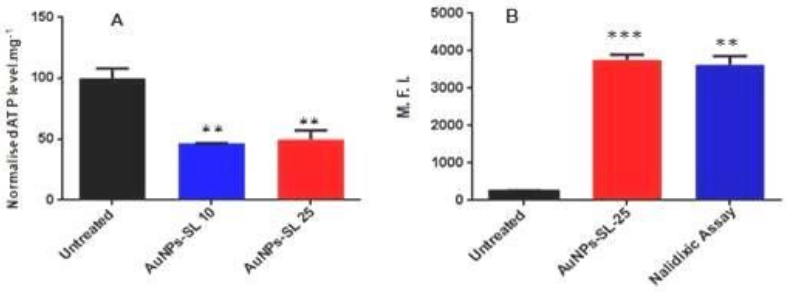

Figure 5

Relative ATP measurement and TUNEL assay in the presence of AuNPs-SL. **A.** Relative ATP measurement at varying concentrations (10 and 25) of AuNPs-SL nanoparticles. The normalized RLU's (Relative Light Units) are plotted, **B.** Estimation of DNA damage using TUNEL assay upon AuNPs-SL-25 treatment, Nalidixic acid is taken as a positive control. (n=3± SD) **P*<0.01. Data analysis was performed using paired *t*-test.

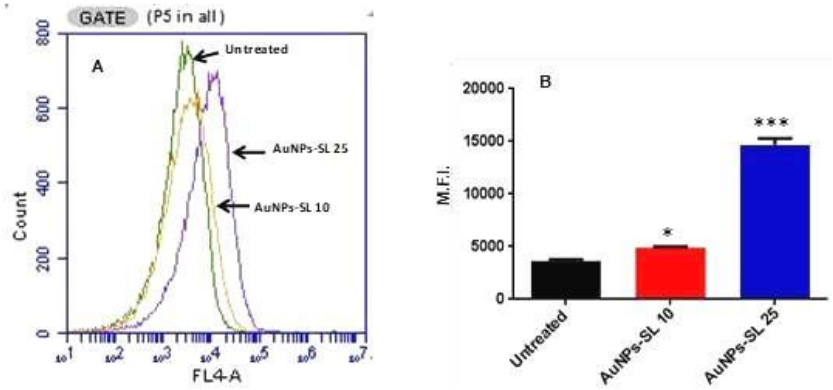

Figure 6

Measurement of apoptosis upon AuNPs-SL treatment using Annexin affinity assay. A. Graphical representation of annexin positive cells at a varying concentration of AuNPs-SL (10 and 25), **B.** MFI of annexin positive cells, (n=3 ± SD). Data analysis is done through paired *t*-test. **P*<0.01, *P*=0.013 for AuNPs-SL-10 and *P*= 0.0008 for AuNPs-SL-25.

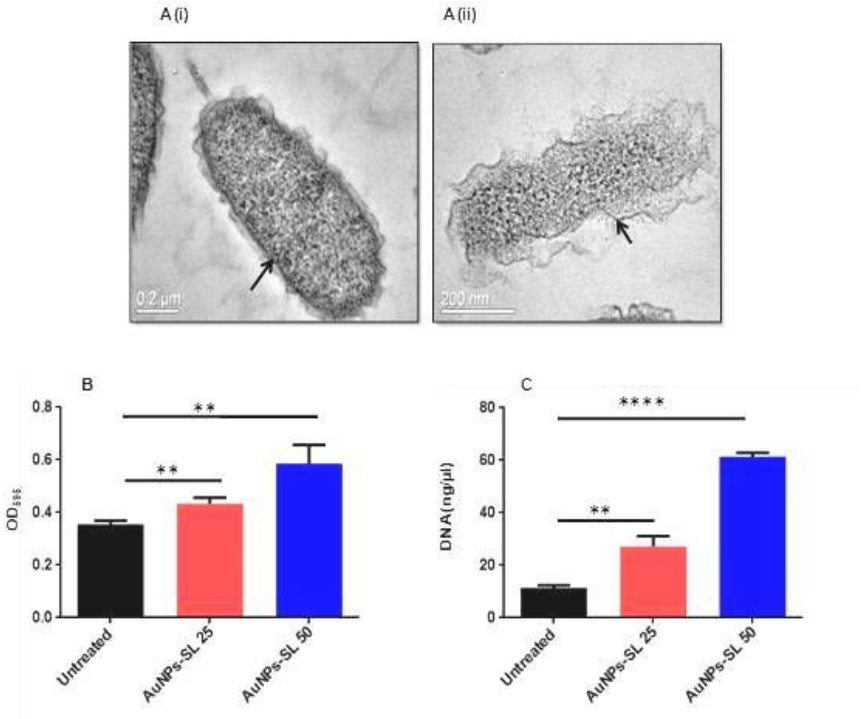

Figure 7

Illustration of membrane damage in the presence AuNPs-SL nanoparticle. **A.** (Ai and Aii) TEM images of *V. cholerae* in the absence (i) and presence of AuNPs-SL (ii). Leakage of protein and DNA (**B and C** respectively**)**. Protein and DNA leakage at a varying concentration of AuNPs-SL (25 and 50) respectively, (n=3± SD). The data was analyzed using Unpaired *t*-test **P*<0.01.

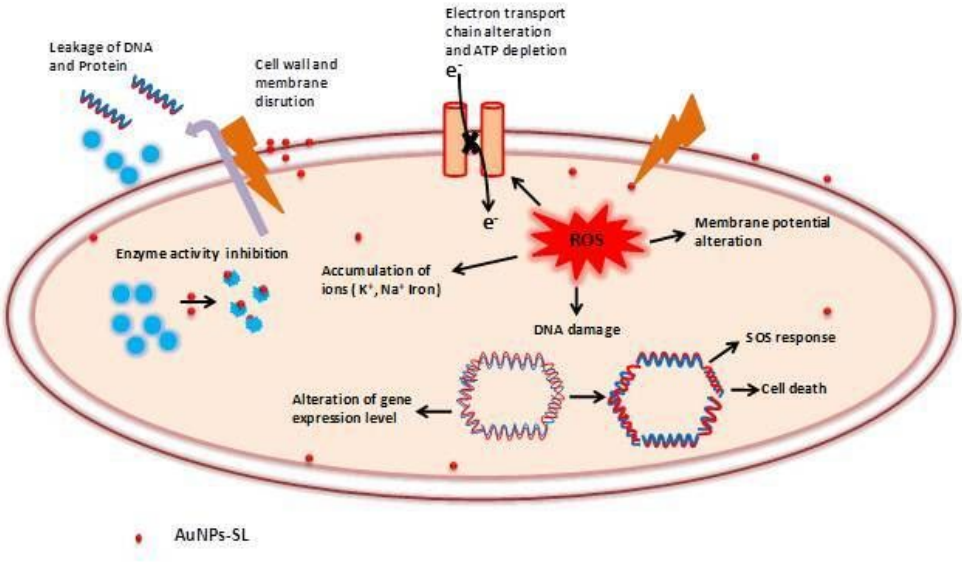

Figure 8

Schematic representation of mechanistic insight of AuNPs-SL mediated killing of *V. cholerae*. The scheme depicts that intracellular accumulation of AuNPs-SL nanoparticles induces ROS formation which further leads to oxidative damages to proteins and DNA and perturbed metal ion homeostasis. Besides that, AuNPs-SL interacts with the membrane and causes membrane damage that further causes alteration in membrane potential, proton motive force. The alteration in PMF and membrane potential deplete intracellular ATP. The intracellular contents of the cell (protein and DNA) also leak-out through the damaged membrane.

Supplementary Files

This is a list of supplementary files associated with this preprint. Click to download.

- SupplementaryInformation31032022format13.doc